*Sensors and Materials*, Vol. 11, No. 6 (1999) 359–367
MYU Tokyo

S & M 0379

# Fabrication of 3-D Microcoils with Ferromagnetic Cores Using a Standard CMOS Process

Lungjieh Yang, Kuangyeu Hsieh[1], Jinghung Chiou[2],
Jennyi Chen[2], Chienliu Chang[2] and Peizen Chang[2]

Department of Mechanical Engineering, Tamkang University, Taiwan
[1]Institute of Material Science and Engineering, National Sun Yat-sen University, Taiwan
[2]Institute of Applied Mechanics, National Taiwan University, Taiwan

(Received July 5, 1999; accepted August 10, 1999)

***Keywords:*** high-permeability material, CMOS, permalloy

Three-dimensional (3-D) micro-closed coils with high-permeability-material cores are fabricated by a complementary-metal-oxide-semiconductor (CMOS) process. Two micromachined integrated inductive components (bar type and ring type) are realized on silicon wafers. In addition, a high-permeability material is electroplated in place of Al-Si-Cu alloy in the triple-metal CMOS structure. In the 3-D structure, a 0.42-$\mu$m-high Ni-20%Fe permalloy magnetic core is wrapped with CMOS conductor lines. Applying the commercial CMOS process to improve conventional CMOS inductive components is of priority concern.

## 1. Introduction

Magnetic materials have been increasingly used for inductive components.[1] Related applications include distributed power supplies for electronic systems or multichip modules, as well as consumer products such as cellular telephones.[2–6] Desirable characteristics of magnetic cores for inductive components such as integrated power inductors and transformers[7–9] can be summarized as follows: first, high saturation in order to obtain high saturation current; second, high permeability to obtain high inductance; third, high resistivity to reduce eddy current loss.

With the standardization of the CMOS process, the thickness and material properties of conduction layers have become fixed. Owing to the behavior of Al-Si-Cu alloy in the CMOS process, the use of the CMOS process to fabricate inductive components does not yield satisfactory performance. For example, CMOS conduction layers used as inductors and transformers have high resistivity and small thickness, resulting in too low a Q factor. In addition, eddy current also causes large loss via the silicon substrate.

Novel micromachining techniques have replaced the conventional microstructure fabrication methods in recent years. These micromachining techniques have facilitated several methods of building microstructures according to different functions. In this study, multilevel conductor coils wrapped around a magnetic core of high-permeability material, Ni-20%Fe, are realized on a silicon wafer, by using metal interconnection techniques, chemical etching in microchannels, and microelectroplating. Results of this work indicate that replacing the conduction layers of CMOS structures makes them compatible with 3-D closed coils.

## 2. Design

The CMOS 0.6 $\mu$m single-polysilicon-triple-metal (SPTM) process developed by Taiwan Semiconductor Manufacture Company (TSMC) has three metallic layers available for the easy fabrication of 3-D microstructures. Figure 1 illustrates the configuration of the CMOS 0.6 $\mu$m SPTM structure. Each metal is isolated by silicon dioxide. Figure 2 shows that each metal layer consists of Ti, Al-Si-Cu alloy and TiN material. Therein, Ti, Al-Si-

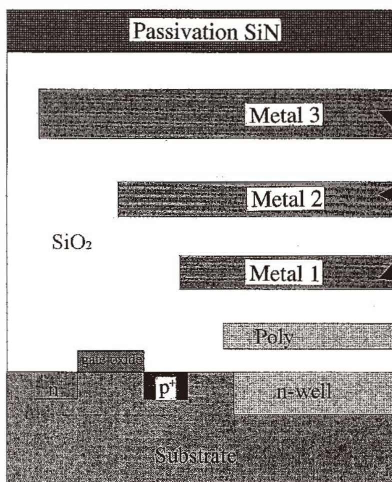


Fig. 1. Structural configuration of CMOS SPTM structure.

Fig. 2. Profile of each metal layer.

Cu alloy, and TiN are used as an adhesion layer, a conduction layer, and an antirefraction layer, respectively. The total thickness of Metal 2 is 5,700 Å. A microchannel space prepared for the magnetic core is achieved by using Al etchant to remove the TiN and Al-Si-Cu alloy.[10] Then, the remaining Ti is later used as a seeding layer for electroplating Ni-20%Fe.

The inductive component consists of a magnetic core and multilevel interconnections. A multilevel metallization scheme is used to wrap the magnetic core with the conductor coils on a planar surface. Metal 1, Metal 3, and the plug-via are used to route N turns of the closed coils with Metal 2 as the magnetic core. The geometrical configurations are illustrated in Figs. 3 and 4. The IC computer-aided-design software, Cadence, can generate the layout of this design.

Figures 5 and 6 show the layouts of the bar-type and ring-type 3-D micro-closed coils, respectively. All designs use the "full custom" design procedure. In bar types, the widths range from 10 $\mu$m to 40 $\mu$m at 10 $\mu$m intervals, and the lengths range from 100 $\mu$m to 300 $\mu$m at 100 $\mu$m intervals. In ring types, the inner radii range 50 $\mu$m to 90 $\mu$m at 10 $\mu$m intervals. All designs of the 3-D micro-closed-coil inductive components correspond to the IC design rule.

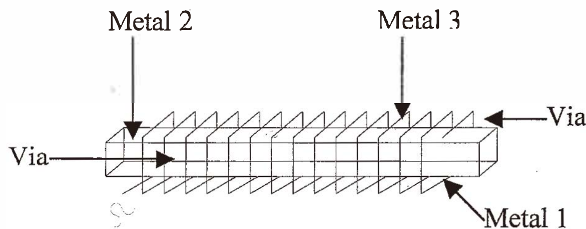


Fig. 3. Bar-type 3-D micro-closed coils.

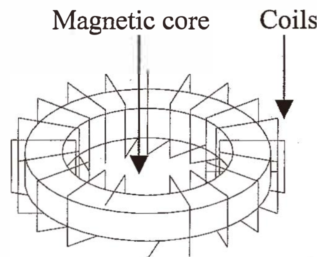


Fig. 4. Ring-type 3-D micro-closed coils.

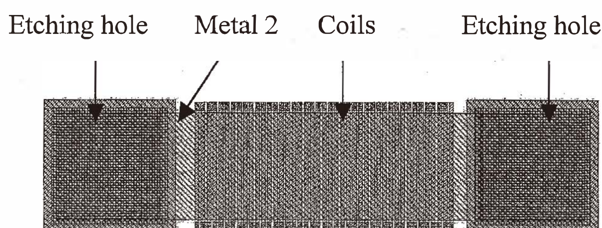


Fig. 5. Layout of the bar-type 3-D micro-closed coil with a width of 40 $\mu$m and length of 100 $\mu$m.

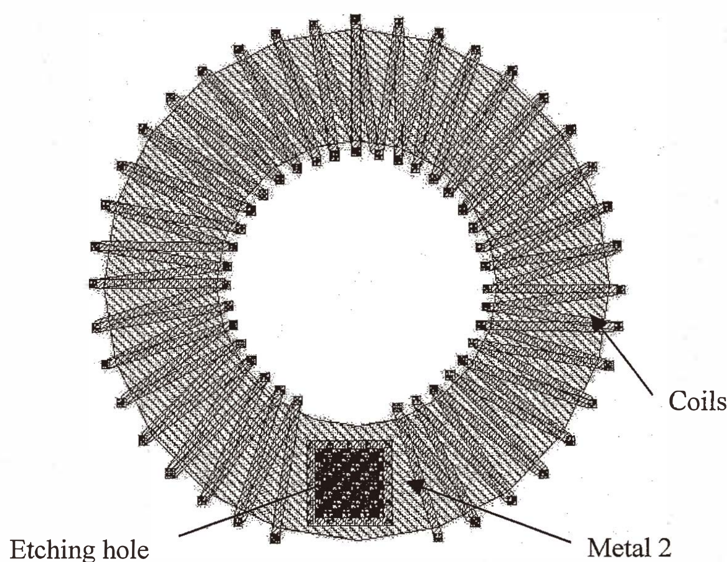


Fig. 6. Layout of the ring-type 3-D micro-closed coil with inner radius of 50 $\mu$m and outer radius of 90 $\mu$m.

## 3. Fabrication

Following checking of the layout and design rule of 3-D micro-closed coils, the CMOS process can be used as a foundry procedure. Next, a microchannel is achieved by using Al etchant to remove the TiN and Al-Si-Cu alloy of Metal 2,[10] after which Ti is used as a seeding layer for electroplating. High-permeability material, Ni-20%Fe, is then electroplated to fill the microchannel space which Metal 2 originally occupied. Figure 7 shows the procedure of the postprocess: (a) the structure of the 3-D micro-closed coils formed by the CMOS 0.6 $\mu$m SPTM process; (b) the coating of the photoresist-S1813 to protect the

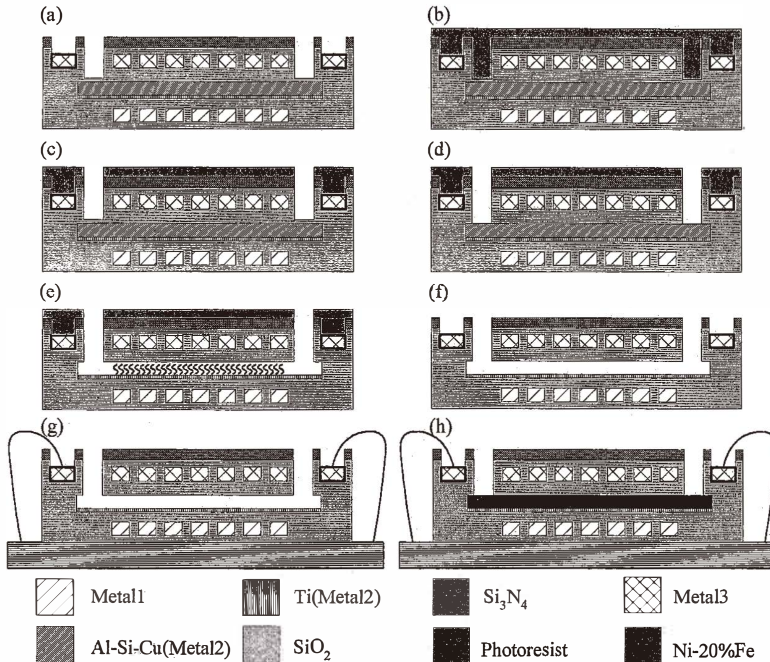


Fig. 7. Flowchart of the postprocess for coils with magnetic cores.

electrical pads of electroplating; and (c) the lithography used to open the etching hole. According to Fig. 7(d), silicon dioxide is etched to TiN of the Metal 2 layer by reactive-ion etching (RIE). The etching conditions are RF power: 117 W, pressure: 30 mTorr, gas flow: 16.8 sccm, and etchant gas: $CF_4$, with an etching rate of 330 Å/min. Figure 7(e) shows the removal of TiN and Al-Si-Cu alloy of Metal 2 by wet etching. The agent is Al etchant. The composition of the Al etchant is 6 $H_3PO_4$: 2 $H_2O_2$: 1 $HNO_3$ and the etching rate is 100 $\mu$m/h (60°C). Figure 7(f) shows the critical-drying method used to dehydrate the dry microchannel. Figure 7(g) shows the bonding wires connecting the electrical pads with the printed circuit board underneath. Figure 7(h) shows the electroplating of the high-permeability material, Ni-20%Fe. The electroplating equipment conditions are a temperature of 50°C, a current of 0.08 A, and an electroplating time of 2 min.

## 4. Results

Figure 8 shows the two types (bar type and ring type) of coil structure obtained after the CMOS process. In the bar-type coils, the line width is fixed at 40 $\mu$m. The coil lengths of the three designs are 100 $\mu$m, 200 $\mu$m, and 300 $\mu$m. Each coil structure has two etching

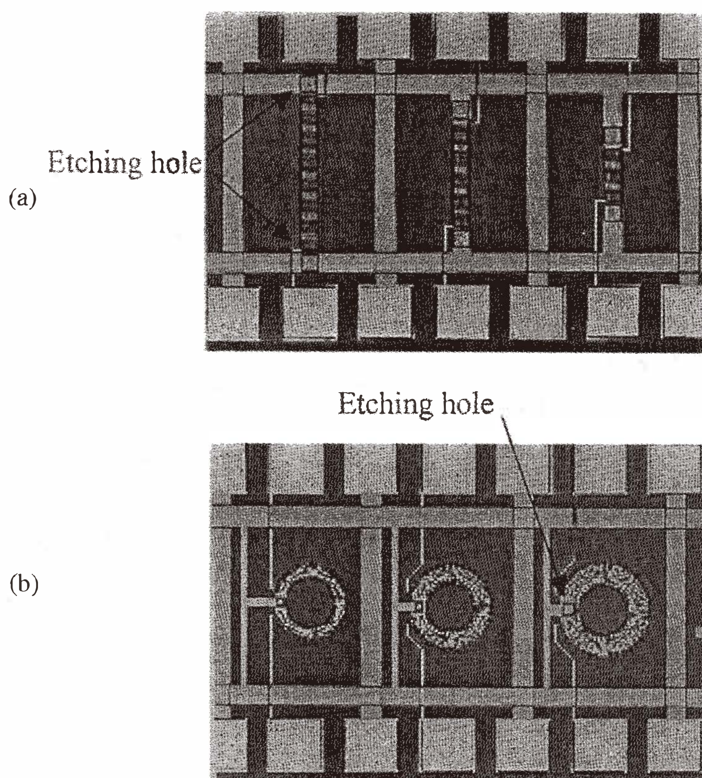


Fig. 8. The 3-D micro-closed coils with a core of Metal 2, formed by CMOS process. (a) Bar-type core. (b) Ring-type core.

holes which are 40 $\mu$m square. Similarly, for the ring-type coils, the inner radius is fixed at 50 $\mu$m. The outer radii are 60 $\mu$m, 70 $\mu$m, and 80 $\mu$m. Each structure has a corresponding etching hole of 20 $\mu$m, 30 $\mu$m and 40 $\mu$m square. Figure 9 shows how TiN and Al-Si-Cu alloy of Metal 2 are removed using Al etchant. The etchant etches TiN and Al-Si-Cu alloy via the etching holes. Obviously, the Ti layer is still not attacked in the microchannel.

When TiN and Al-Si-Cu alloy of Metal 2 are etched by Al etchant, a 0.42-$\mu$m-high microchannel is made, leaving only the Ti layer of Metal 2. The solution of Ni-20%Fe is allowed to flow into the etching hole of the microchannel. The use of the Ti layer as an electroplating seeding layer allows the Ni-20%Fe to be deposited over it. Figure 10 indicates that a short and wide bar-type microchannel can lead to more uniform electroplating results than a long and narrow bar-type microchannel. This is because the solution of Ni-20%Fe easily permutes in electroplating. As seen in Fig. 11, the ring-type microchannel has only one etching hole; not only is the etching rate slower than that of the bar type, but it is also difficult for the electroplating solution to permute, ultimately causing some area of the microchannel to not be electroplated.

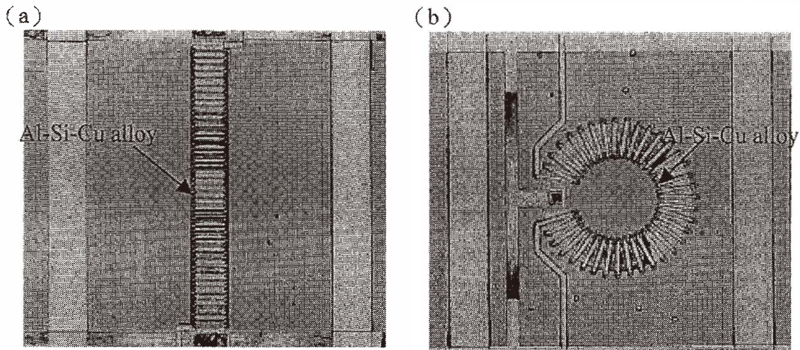


Fig. 9. Etching of TiN and Al-Si-Cu alloy of Metal 2. (a) Bar-type microchannel. (b) Ring-type microchannel.

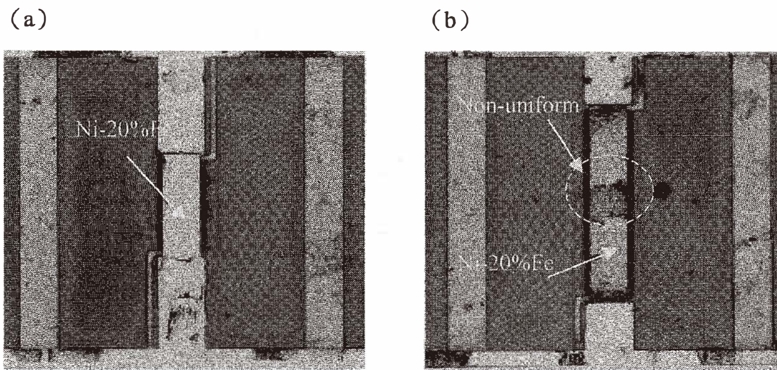


Fig. 10. Results of electroplating. (a) Bar-type core with width of 40 $\mu$m and length of 100 $\mu$m. (b) Bar-type core with width of 40 $\mu$m and length of 200 $\mu$m.

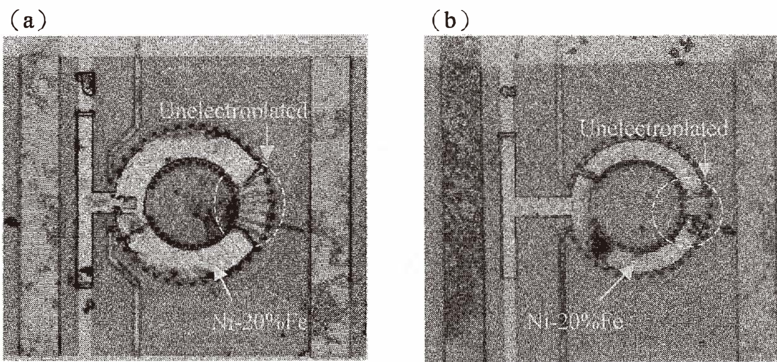


Fig. 11. Results of electroplating. (a) Ring-type core with inner radius of 50 $\mu$m and outer radius of 90 $\mu$m. (b) Ring-type core with inner radius of 50 $\mu$m and outer radius of 80 $\mu$m.

## 5. Discussion

The bar-type coil has two etching holes, which explain why the etching rate of Al-Si-Cu alloy is faster than with the ring-type coil. In addition, the good permutation of electroplating solution through the bar-type coils is superior to the case of the ring-type coils with one etching hole only. Experimental results indicate that for the bar type, a short, wide structure is more suitable for electroplating. In the ring type, two etching holes can be used to improve the electroplating effect. We successfully electroplated Ni-20%Fe alloy in microchannels with lengths of 100 $\mu$m to 300 $\mu$m, widths of 10 $\mu$m to 40 $\mu$m, and a height of 0.42 $\mu$m.

As is generally known, using CMOS spiral inductors to predict the Q factor and inductance of inductors is extremely difficult. Silicon substrate loss is the most important parameter affecting the Q factor. In the design proposed herein, the layouts of inductors that are formed as helical and toroidal closed coils can minimize the leakage flux around the individual turns of the wire. This feature significantly reduces silicon substrate loss and hence increases the Q factor. In addition, applying the postprocess to electroplate a high-permeability material, Ni-20%Fe, in the coils increases the inductance. Furthermore, the proposed design requires a considerably smaller area than the conventional spiral inductors having the same inductance.

## 6. Conclusions

In this work, fully integrated micromachined inductive components with magnetic cores, Ni-20%Fe 0.42 $\mu$m thick, are realized on silicon wafers. The etching selectivity of Al-Si-Cu is high and the Ti layer is not destroyed. Therefore, the Ti layer is highly recommended for use as an electroplating cathode. Execution of electroplating depends on the geometrical configuration of the structure such as the length and width of the channel structure and the number of etching holes; the optimal case is the bar-type coil with a width of 40 $\mu$m, length of 100 $\mu$m and two etching holes of 40 $\mu$m square. Replacing the conduction layers of the CMOS structure makes the 3-D closed coils and CMOS structural layers compatible with each other. These techniques can be used for micro-inductive devices such as inductors and transformers.

**Acknowledgements**

The authors would like to thank Dr. L. P. Chen, Y. P. Ho, and D. C. Lin of National Nano-Device Lab (NDL) for their valuable assistance with the measurements. The National Chip Implementation Center (CIC) is also appreciated for the foundry support. We are grateful to the Solid-State Group of the Department of Electrical Engineering at National Taiwan University, for allowing us to use their valuable equipment. Microsystem Laboratory of Industrial Technology Research Institute is also appreciated for their valuable assistance in using the electroplating technology.

## References

1 J. A. Rogers, R. J. Jackman and G. M. Whitesides: J. Microelectromechanical Systems **16** (1997) 184.
2 M. Soyuer, K. A. Jenkins, J. N. Burghartz and H. A. Ainspab: IEEE J. Solid-State Circuits **31** (1996) 2.
3 J. N. Craninckx and M. S. J. Ssteyaert: IEEE J. Solid-State Circuits **30** (1995) 12.
4 F. Mernyei, F. Darrer, M. Pardoen and A. Sibrai: IEEE Microwave and Guided Wave Letters **8** (1998) 9.
5 J. Craninckx and M. S. J. Ssteyaert: IEEE J. Solid-State Circuits **32** (1997) 5.
6 K B. Ashby and I. A. Koulias: IEEE J. Solid-State Circuits **31** (1996) 1.
7 J. Y. Park and M. G. Allen: Electronic Components and Technology (IEEE, 1996) 375.
8 C. H. Ahn, Y. J. Kim and M. G. Allen: IEEE Trans. Components Packaging Manufacturing **17** (1994) 463.
9 H. Yoda, S. Kurashima, M. Endoh and N. Wakatsuki: IEEE Trans. Magnetics **25** (1989) 3821.
10 K. R. Williams and R. S. Muller: J. Microelectromechanical Systems **5** (1996) 156.